Structural, Electronic and Optical Properties of $Sc_xAl_{1-x}N$ alloys within DFT Calculations

Asma Said*, Yasmina Oussaifi, Moncef Said

Laboratoire de la matière condensée et nanosciences, Département de physique, Faculté des sciences de Monastir, Monastir, Tunisie
Email: *saidasma1987@yahoo.fr

Abstract

Structural, electronic and optical properties of Sc-based aluminum-nitride alloy have been carried out with first-principles methods using both local density approximation (LDA) and Heyd-Scuseria-Ernzerhof (HSE) hybrid functional. This latter provides a more accurate description of the lattice parameters, enthalpy of formation, electronic and optical properties of our alloy than standard DFT. We found the transition from wurtzite to rocksalt structures at 61% of Sc concentration. By increasing the scandium concentration, the lattice parameters and the band gap decrease. The HSE band gap is in good agreement with available experimental data. The existence of the strong hybridization between Sc 3d and N 2p indicates the transport of electrons from Sc to N atoms. Besides, it is shown that the insertion of the Sc atom leads to the redshift of the optical absorption edge. The optical absorption of $Sc_xAl_{1-x}N$ is found to decrease with increasing Sc concentrations in the low energy range. Because of this, $Sc_xAl_{1-x}N$ have a great potential for applications in photovoltaics and photocatalysis.

Keywords

DFT, Electronic and Optical Properties, ScAlN, Hybrid Functional HSE

1. Introduction

Recent theoretical [1] [2] and experimental [3] [4] researches show that ScN is a promising material for medium and high temperature thermoelectric applications. It has suitable thermal and electrical properties for thermoelectric application, such as high melting point (2900 K) [5]. Due to its high temperature stability, this material is promising for high-temperature piezoelectric devices. These properties allow the ScN to be incorporated directly into III-nitride structures [6] and to growth successfully using a wide range of

techniques in the context of lighting industry and other emerging applications, in order to improve device performance. For these reasons, the incorporation of scandium into aluminum nitride gives an emerging semiconductor material, with potential applications in optics and electronics due to its unique properties.

Notice that wurtzite ScAlN is presented as an alternative to InAlN for optoelectronic applications operating in the 200 - 550 nm range [7] Several experimental [8] and theoretical [9] studies have been postponed to explore the properties of this alloy.

For this purpose, using LDA and HSE functional method which is less computationally demanding compared to PBE0, we have made a complete theoretical study of ScAlN alloy in the wurtzite and rocksalt. We focus on structural, electronic and optical properties cause till now we haven't found a complete theoretical study of electronic and especially optical properties of this compound except reference [10] which has shown a brief study of these properties using only GGA approximation.

This paper is organized as follows: after an introduction, we describe in Section 2, the computational details. In Section 3, we present and discuss the main results obtained from this study. The conclusions drawn from this study are summarized in Section 4.

2. Computational Methods

The point of departure of our calculations is density functional theory (DFT) in the local density approximation (LDA) with the parameterization of Perdew and Zunger [11]. We used the QUANTUM-ESPRESSO package [12] together with norm-conserving pseudopotentials and Trouiller-Martins [13] to report the interactions between ionic cores. The simulation procedure is iterated self-consistency with the cutoff energy of 80 and 60 Ry and a k-points grid of 6 × 6 × 6 and 12 × 12 × 6 in the reciprocal space for the rocksalt and wurtzite structures, respectively. It is notorious that the LDA leads to an underestimation of the lattice constants and band gaps [14] [15]. The cause of this inaccuracy is due to the systematic error in the treatment of exchange in the exchange-correlation energy (XC). A manner to overcome this shortfall is to use Heyd-Scuseria Ernzerhof hybrid-functionals where part of the nonlocal Hartree-Fock (HF) type exchange is mixed with a functional semilocal XC [16] giving the following equation:

$$E_{xc}^{HSE} = \alpha E_X^{HF,SR}(\omega) + (1-\alpha)E_X^{SR}(\omega) + E_X^{IR}(\omega) + E_c \tag{1}$$

where α is the mixing coefficient and ω is the screening parameter that controls the decomposition of the Coulomb kernel into short-range(SR) and long-range (LR) exchange contributions.

To lead a new orientation of the effect of Sc on the AlN system for the various concentrations, theoretical research remains essential. However, few theoretical studies, with LDA and GGA, have been investigated for this compound. Notably,

The local density approximation (LDA) or generalized gradient approximation (GGA) to density functional theory (DFT) limits the theoretical understanding of the electronic and optical properties of such materials owing to the fact that they heavily underestimate the band gaps of semiconductor compounds. Also, these approximations (LDA, GGA) impart typically large errors in the calculated formation energies and the position of transition levels. This is particularly in the case of wide band gap materials, and in materials that are intended to have no gap in LDA. Various approaches have been suggested to surmount this discord, such as LDA/GGA + U and hybrid functional. For LDA + U, it enhances the description of the bands related to the semi-core d states, which provides only partial correction band gaps in materials such as ScN and InN [17]. As though the LDA problem linked to the discontinuity of the exchange-correlation potential as a function of the number of electrons still persists. Although, Hybrid functional, such as HSE and PBE0 [18], comprise a part of Hartree-Fock (HF) type change in the exchangeable functional correlation (XC), only within a fixed radius (screening length), offer a major improvement of the LDA-GGA description of the structure and electronic properties of many materials [18] [19] [20]

In this work, we have used the HSE, for it is less computationally demanding compared to PBE0 [21].

3. Result and Discussion

3.1. Lattice Parameters and Stability

The computed cell parameters using LDA and HSE functional for both AlN and ScN structures are presented in Table 1 together with the available theoretical and experimental results. As shown in Table 1, the calculated lattice parameters are in reasonable agreement with experimental and theoretical values, within 3% and 1% for LDA and HSE, respectively.

AlN is known to stabilize in wurtzite structure while ScN is the rocksalt one. Our computational results of $Sc_xAl_{1-x}N$ ($0 \leq x \leq 1$) lattice constants using both functional (LDA and HSE) are shown in Figure 1. It can be seen that the variation

Table 1. LDA and HSE calculated lattice parameters for binaries AlN and ScN in both rocksalt and wurtzite structures compared with available experimental and theoretical results.

		a(Å)				c/a			
		LDA	HSE	Oth. Cal.	Exp.	LDA	HSE	Oth. Cal.	Exp.
AlN	RS	4.01	4.04	4.05 [22], 4. 02 [23]	4.05 [24]	-	-	-	-
	WZ	3.08	3.10	3.10 [25]	3.11 [26]	1.63	1.61	1.62 [25]	1.60 [26]
ScN	RS	4.40	4.45	4.45 [22]	4.50 [27]	-	-	-	-
	WZ	3.54	3.55	3.54 [22], 3.50 [28]	-	1.58	1.64	1.57 [22], 1.60 [28]	-
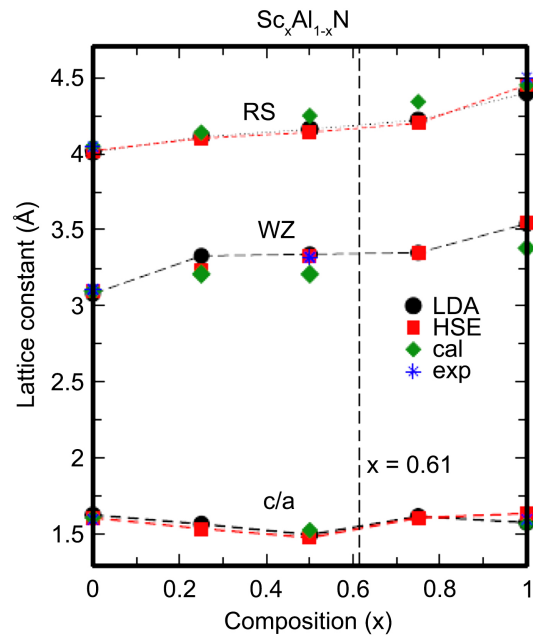
Figure 1. Lattice parameters as a function of scandium composition.

of the lattice parameters of the ternary alloy in both rocksalt and wurtzite structures, as a function of the scandium composition are not important, the same behavior is seen for the c/a lattice parameter which may be attributed to the difference in atomic radii of Sc and Al atoms and to the small difference between the lattice parameters of the binary compounds.

To understand the behavior of stability of this alloy, the study of thermodynamic properties is essential, in particular as regards enthalpies of formation. AlN and ScN are stable in the wurtzite and rocksalt phases, respectively. The mixing enthalpy (H_{mix}) of $Sc_xAl_{1-x}N$ alloy with different phases can be expressed as:

$$H_{min}\left(Sc_xAl_{1-x}N\right) = E\left(ScN, Rocksalt\right) - \left(1-x\right)E\left(AlN, wurtzite\right) \qquad (2)$$

where E is the total energy per unit cell of the bulk compound x and (1 − x) are the ScN and AlN mole fraction, respectively.

Hoglund *et al.* [29], using first-principles calculations, have calculated the lattice parameters and mixing enthalpies of cubic, wurtzite and hexagonal $Sc_xAl_{1-x}N$ and they found the transition from cubic to wurtzite structures at x = 0.45, which deviates from the experimental results (x = 0.60) [29].

The obtained results with HSE functional of the mixing enthalpy (H_{mix}) of $Sc_xAl_{1-x}N$ alloy with, rocksalt (RS) and wurtzite (WZ) phases are presented in **Figure 2**. The ternary alloy changes from hexagonal to cubic when the ScN mole fraction exceeds 0.61 fractions. This value is consistent with the observed experimental result (x = 0.6) [29]. As a result of this, the calculated result fall in the vicinity of the stable region from the experimental and makes the HSE functional more consistent with the experimental data.
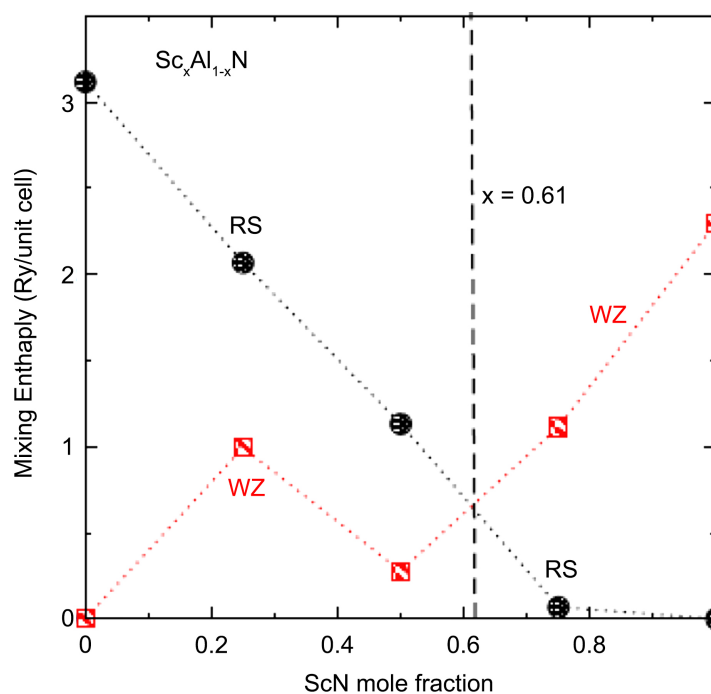
Figure 2. Mixing enthalpies in wurtzite and rocksalt phases.

3.2. Electronic Properties

The calculated band gaps of the binaries constituents in WZ and RS structures are tabulated and compared with the experimental values in **Table 2**. We display in **Figure 3** the obtained energy gaps of $Sc_xAl_{1-x}N$, using LDA, HSE and compared them with experimental and other theoretical results. A decrease in band gap with increasing Sc content is observed experimentally [8]. Our results obtained with LDA are in good agreement with other LDA-theoretical results, although notably smaller than those obtained experimentally. For example, the LDA band gaps of RS and WZ-AlN are 4.32 eV and 4.23 eV which in agreement with Jiao [30] and Berkok [23] respectively. The same for RS and WZ-ScN are 0.10 eV and 2.9 eV which in accordance with other LDA-theoretical results [8] [23] [35], but underestimated by about 1 eV compared to the experimental values.

To surmount this problem, we have used the standard HSE hybrid functional (α = 25). The band gap values determined by the hybrid functional are significantly improved and the discrepancy with experiment results is about 2%. Whereas, those calculated by the standard DFT are about 10% smaller than the experimental values. Our results demonstrate well, that HSE emerges as an appropriate method for the study of electronic properties of semiconducting alloys.

Recently, Deng *et al.* [8] demonstrated that the optical absorption of hexagonal $Sc_xAl_{1-x}N$ indicates a band gap of 6.15 - 9.32 x eV for 0 < x < 1 and a linearly increasing density of defect states within the gap. The average bond angle decreases linearly with x, suggesting a trend towards the metastable hexagonal-ScN structure. Zhang *et al.* [38] noted that the Wurtzite-structure ScAlN alloy is a wide band-gap semiconductor, which can be stabilised at low Sc contents.

Table 2. LDA and HSE calculated band gaps for binaries AlN and ScN in both rocksalt and wurtzite structures compared with available experimental and theoretical results. (DG and IG denoted direct or indirect gap, respectively).

		E_g (eV)			
		LDA	HSE	Oth. Cal.	Exp.
AlN	RS(IG)	4.32	4.40	4.47 [30], 5.82 [31]	4.40 [32]
	WZ(DG)	4.23	5.45	4.62 [23]	6.28 [33]
ScN	RS(IG)	0.10	1.30	−0.15 [23], −0.19 [34]	1.30 [36]
	WZ(IG)	2.90	3.20	2.91 [23], 2.90 [35]	3.50 [37]
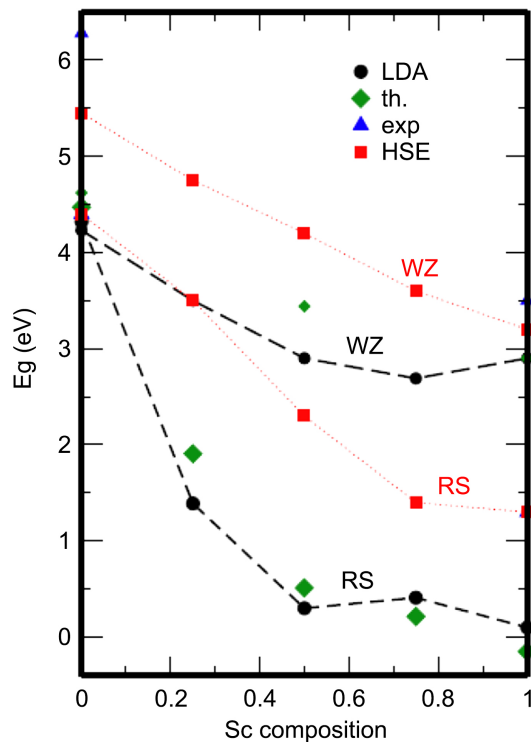
Figure 3. Energy band gap versus Scandium content.

In order to get a better understanding of the electronic structure of the investigated compounds, we display in **Figure 4** the total densities of states (TDOS) of $Sc_xAl_{1-x}N$ for both structures.

Note that the valence band states of intrinsic AlN are composed of two main parts: the upper part which is primarily derived from N s orbitals and the lower part which is mainly due to the N p orbitals for both RS and WZ structures. Once the Sc composition increases, we note that the peak in the lowest valence band increases. Also, the conduction band gradually shifts towards low energies.
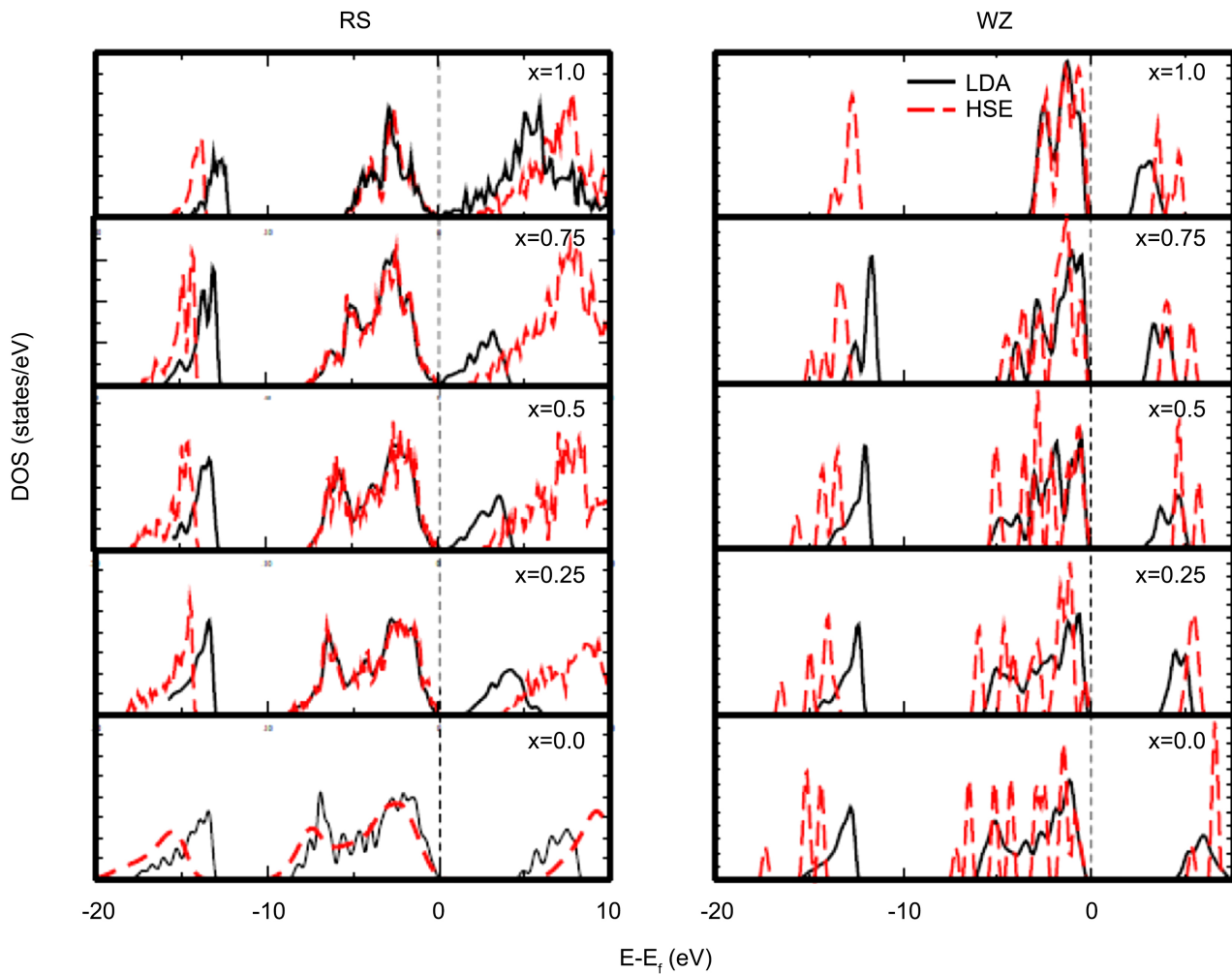
Figure 4. LDA and HSE calculated of total densities of states (TDOS) of ScAlN in wurtzite and rocksalt phases.

Using HSE functional, we note a blue shift of the conduction band minima in the case of WZ-ScN and an appearance of a valence band located at about −12 eV. Likewise, we note a widening of the gap.

To further study the electronic properties, the partial densities of states of $Sc_xAl_{1-x}N$ alloy are shown in **Figure 5**. We note that, the top of the valence band and the bottom of the conduction band are mainly composed by the N-2p states and Sc-3d states, respectively. The strong hybridization between Sc-d and N-p indicates the transfer of electrons from Sc atoms to N atoms and their participation in the ionic bonding between Sc and N atoms. The incorporation of Sc atom largely affects the electronic states of neighboring N atoms.

3.3. Optical Properties

In the following, the optical properties of Sc-ordered AlN systems will be systematically discussed on the basis of dielectric function, absorption coefficient and refractive index. All the results are presented with the polarization vectors perpendicular to the c-axis.
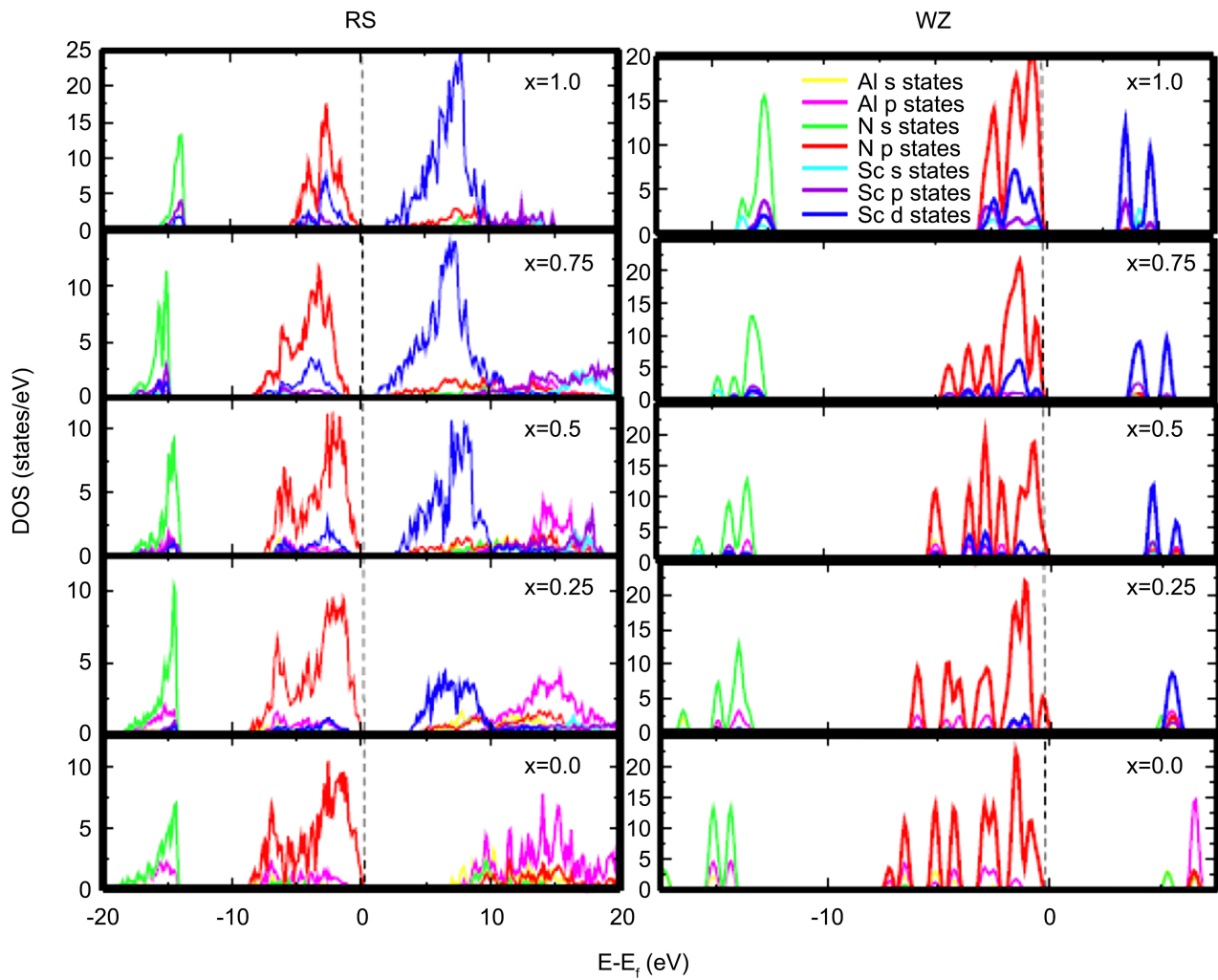
Figure 5. The HSE partial densities of states (PDOS) of ScAlN in wurtzite and rocksalt phases.

The complex dielectric constant ε is defined by $\varepsilon = \varepsilon_1 + i\varepsilon_2$. The imaginary part of the dielectric function is completed within the electric dipole approximation equation. The real part can be assessed from the imaginary part by using the Kramer-Kronig relations and given in our recent paper [39] as follows:

$$\varepsilon_2(\omega) = \frac{\pi}{\varepsilon_0}\left(\frac{e}{m\omega}\right)^2 \times \sum_{V,C}\left\{\int_{BZ}\frac{2dK}{(2\pi)^3}\left|a \cdot M_{CV}(K)\right|^2 \times \delta\left[E_C(K) - E_V(K) - \hbar\omega\right]\right\}$$

(3)

$$\varepsilon_1(\omega) = 1 + \frac{2e}{\varepsilon_0 m^2}\sum_{V,C}\int_{BZ}\frac{2dK}{(2\pi)^3}\frac{\left|a \cdot M_{CV}(K)\right|^2}{\left[E_C(K) - E_V(K)\right]} \times \frac{\hbar^3}{\left[E_C(K) - E_V(K)\right]^2 - \hbar^2\omega^2}$$

(4)

Figure 6 illustrates the HSE calculated of the imaginary part $\varepsilon_2(\omega)$ for AlN, ScN and $Sc_xAl_{1-x}N$. For AlN, there are three major peaks located at 4.30 eV, 7.50 eV and 8.50 eV and two main peaks located at 9.11 eV and 12 eV for the wurtzite and roksalt structures, respectively. These results are in agreement with the
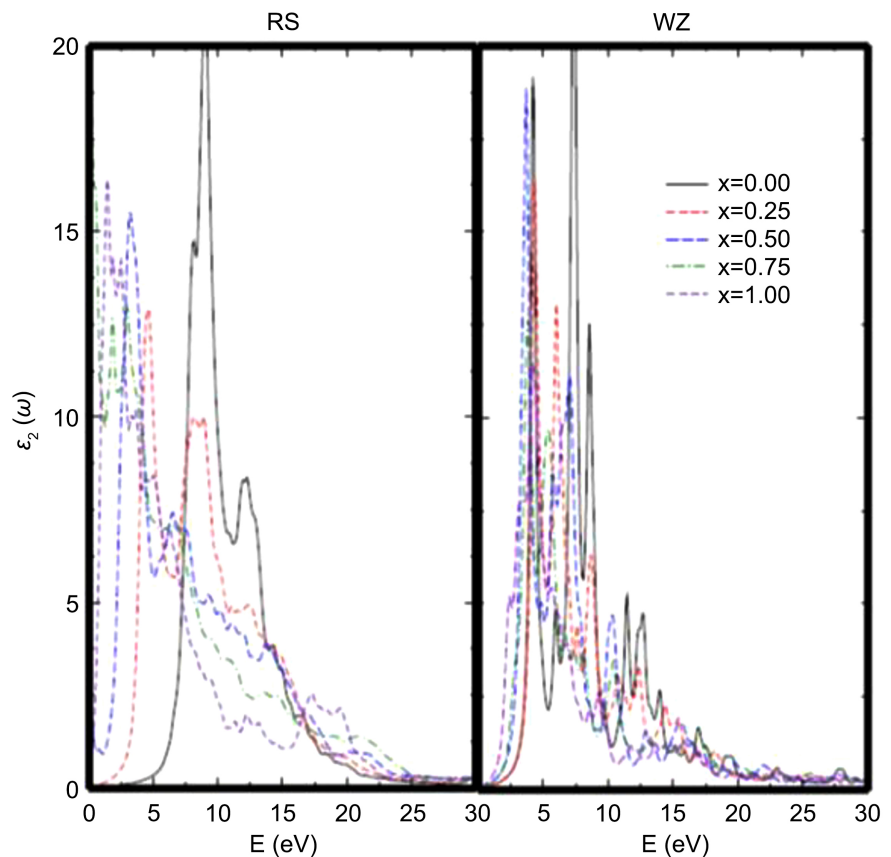
Figure 6. The HSE imaginary part $\varepsilon_2(\omega)$ of the dielectric function for Sc-doped AlN.

available experimental results [40]. The first peak (4.3 eV for WZ and 9.11 eV for RS structures) should be mainly due to the interband transitions, between N-2p orbitals in the highest valence band and Al-3p in the lowest conduction band. The second peak is mainly due to the interband transitions from N-2s and Al-2p orbital as seen in the DOS given in **Figure 5**.

By increasing Sc concentration, the peaks move to lower energies. This might be strongly dependent on the ionic polarization of the ScAlN crystal due to the large electronegativity of N. For pure ScN, the major peak is at about 2.00 and 4.5 eV, for RS and WZ structures correspondingly, which is mainly derived from the optical transition between the Sc-d states and N-p states.

Our results of ScN rocksalt are in agreement with experimental values [41].

The real parts of the dielectric function $\varepsilon_1(\omega)$ are shown in **Figure 7**. For the binary WZ-AlN, $\varepsilon(0)$ given by the low energy limit of $\varepsilon(\omega)$ is about 4.6 eV, which is in accordance with experimental and other theoretical results (4.61, 4.70 eV [42] [43]). As far as we know, for the RS-AlN and WZ-ScN there are no experimental data available related to the static macroscopic dielectric constants, and this can serve as a prediction for future investigations.

As displayed in **Figure 7**, the ScAlN material presents a similar trend mainly for higher energy, for both WZ and RS structures, which behave like a metallic property above 7.01 eV for WZ-AlN and 3 eV for RS-ScN.
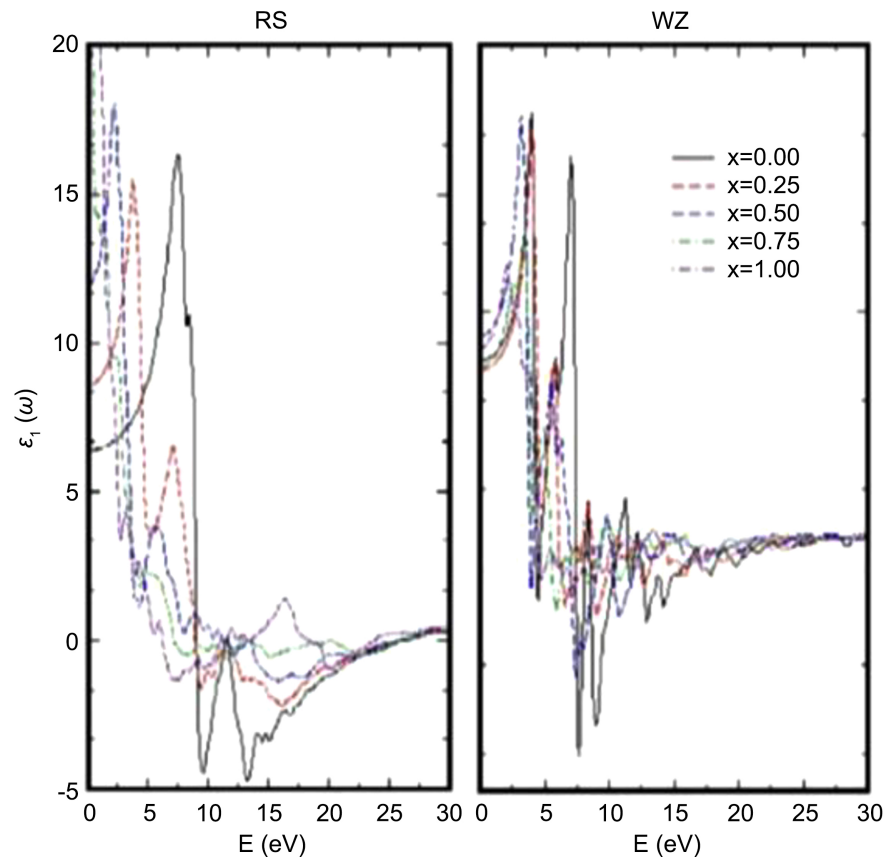
Figure 7. The HSE real part $\varepsilon_1(\omega)$ of the dielectric function for Sc-doped AlN.

The dielectric functions are sufficient to derive other physical properties like the absorption coefficient and refractive index.

For this purpose, we present in **Figure 8**, the optical absorption coefficient of Sc doped AlN alloy. As can be seen, the absorption coefficient decreases with the increase of Sc concentration, in good agreement with the previous calculation. This decrease is mainly ascribed to the reduction of Al p states. It is also clear that the absorption edge of $Sc_xAl_{1-x}N$ alloys shifts evidently to lower photon energies with the increasing Sc doping concentration, compared to that of pure AlN. Our obtained results are in agreement with those of Zhu *et al.* [10]. Moreover, the absorption coefficient of Sc-doped AlN systems decreases with Sc content, as shown in **Figure 8**, which is mainly, ascribed to the effect of Sc 3d states.

The absorption region is quite wide and it is still located in the UV region. The line shape is almost the same for the doped and undoped AlN systems in the high-energy range. Therefore, this material could be employed in optoelectronic devices of short wavelengths, such as UV detector and light-emitting diodes (LEDs). These properties indicate that the concentrations of Sc dopant affect mainly the optical properties specifically in the high energy range.

The refractive index $n(\omega)$ is a very important physical parameter related to microscopic atomic interactions. The knowledge of this index is necessary for accurate modeling and design of devices. Thus, the refraction index, absorption
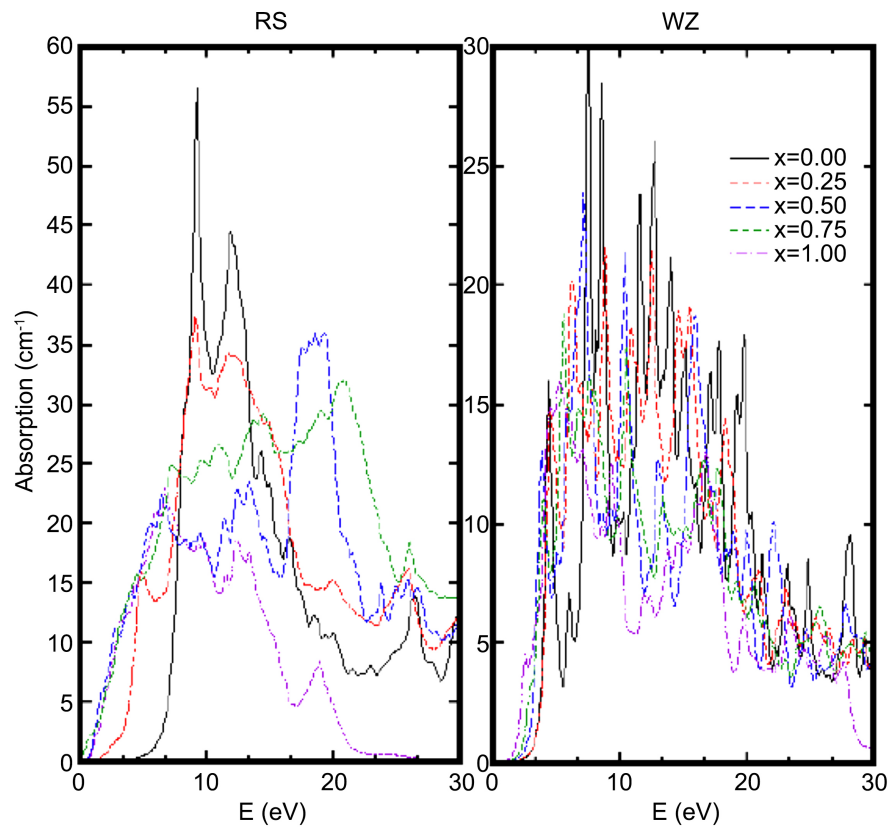
Figure 8. The HSE absorption edge of ScAlN alloys.

coefficient and other optical constants can be obtained [44] [45]. The refraction index is given in Equation (5).

$$n(\omega) = \frac{1}{\sqrt{2}}\left[\sqrt{\varepsilon_1(\omega)^2 + \varepsilon_2(\omega)^2} + \varepsilon_1(\omega)\right]^{\frac{1}{2}} \qquad (5)$$

Figure 9 shows the refractivity index $n(\omega)$ of ScAlN systems in the energy range of 0 - 30 eV. For AlN, the static refractive index $n(0)$ is found to be 3.10 and 2.62 for RS and WZ structures, respectively. It is also noted that the values of $n(\omega)$ increase with the increasing photon energy in the transparency region hit record highs in the ultraviolet at about 7.72 eV and 4.8 eV in RS and WZ phases of AlN, respectively.

Our results are in accordance with other's calculated and experimental results [40]. As can be seen by increasing Sc content, the low photon energy range (<10 eV) is characterized by appreciable refractivity, whereas, in the 12 - 27 eV photon-energy range, the refractivity undergoes a change from the strongest located at to the second weakest. At the photon-energy range of 25 - 30 eV, the refractivity shows an opposite trend.

The imaginary part, absorption edge and refractive index of the rocksalt phase are quite different from those of the wurtzite phase. These results endorsed that either RS or WZ-ScAlN can be a material of choice for optoelectronics and solar cell applications.
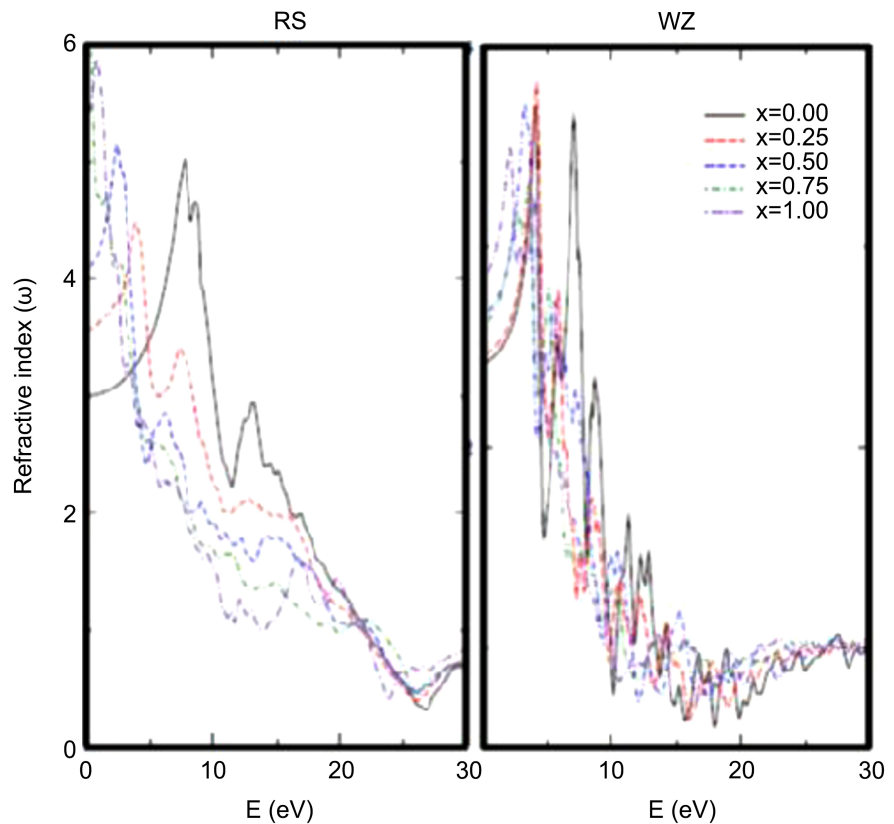
Figure 9. The HSE refractivity index $n(\omega)$ of ScAlN systems.

4. Conclusions

We have presented the fundamental properties of both RS and WZ structures of $Sc_xAl_{1-x}N$ ($0 < x < 1$) using density-functional calculations within LDA and HSE functional. This study reveals that HSE performs well in reproducing the experimental crystal structures, band gap values and mixing enthalpies of $Sc_xAl_{1-x}N$ compounds. Also our calculations show that, the phase transition from WZ to RS is occurred at x = 0.61, in perfect agreement with experimental result. The variation of the lattice constants is almost linear, this latter increases with the increase of the Sc concentration. The band gap decreases with the increase of Sc concentration in the RS phase. In particular, as the Sc concentration increases, the edge of the CB is shifted rightward due to the effects of the 3d shell of scandium.

The absorption edge of $Sc_xAl_{1-x}N$ alloys shifts to lower energy range with increasing Sc doping when compared to the pure AlN. The relations of the optical properties to the interband transitions were also discussed. The calculation details presented here are useful to initiate further experimental investigations and providing a prediction for these materials.

Conflicts of Interest

The authors declare no conflicts of interest regarding the publication of this paper.

References

[1] Lambrecht, W.R.L. (2000) Electronic Structure and Optical Spectra of the Semimetal ScAs and of the Indirect-Band-Gap Semiconductors ScN and GdN. *Physical Review B*, 62, 13538-13545. https://doi.org/10.1103/PhysRevB.62.13538

[2] Gall, D., Städele, M., Järrendahl, K., Petrov, I., Desjardins, P., Haasch, R.T., Lee, T.-Y. and Greene, J.E. (2001) Electronic Structure of ScN Determined Using Optical Spectroscopy, Photoemission, and *Ab Initio* Calculations. *Physical Review B*, 63, Article ID: 125119. https://doi.org/10.1103/PhysRevB.63.125119

[3] Bai, X. and Kordesch, M.E. (2001) Structure and Optical Properties of ScN Thin Films. *Applied Surface Science*, 175-176, 499-504. https://doi.org/10.1016/S0169-4332(01)00165-9

[4] Humphreys, C.J., Moram, M.A. and Barber, Z.H. (2008) The Effect of Oxygen Incorporation in Sputtered Scandium Nitride Films. *Thin Solid Films*, 516, 8569-8572. https://doi.org/10.1016/j.tsf.2008.05.050

[5] Gall, D., Petrov, I., Hellgren, N., Hultman, L., Sundgren, J.E. and Greene, J.E. (1998) Growth of Poly- and Single-Crystal ScN on MgO(001): Role of Low-Energy N_2^+ Irradiation in Determining Texture, Microstructure Evolution, and Mechanical Properties. *Journal of Applied Physics*, 84, 6034-6041. https://doi.org/10.1063/1.368913

[6] Moram, M.A., Zhang, Y., Kappers, M.J., Barber, Z.H. and Humphreys, C.J. (2007) Dislocation Reduction in Gallium Nitride Films Using Scandium Nitride Interlayers. *Applied Physics Letters*, 91, Article ID: 152101. https://doi.org/10.1063/1.2794009

[7] Zhang, S.Y., Holec, D., Fu, W.Y., *et al.* (2013) Tunable Optoelectronic and Ferroelectric Properties in Sc-Based III-Nitrides. *Journal of Applied Physics*, 114, Article ID: 133510. https://doi.org/10.1063/1.4824179

[8] Gall, D., Deng, R. and Evans, S.R. (2013) Bandgap in $A_{1-x}Sc_xN$. *Applied Physics Letters*, 102, 2103.

[9] Matloub, R., Hadad, M., Mazzalai, A., Chidambaram, N., Moulard, G., *et al.* (2013) Piezoelectric $Al_{1-x}Sc_xN$ Thin Films: A Semiconductor Compatible Solution for Mechanical Energy Harvesting and Sensors. *Applied Physics Letters*, 102, Article ID: 152903. https://doi.org/10.1063/1.4800231

[10] Zhu, M., Hua, L. and Xiong, F. (2014) First Principles Study on the Structural, Electronic, and Optical Properties of Sc-Doped AlN. *Russian Journal of Physical Chemistry A*, 88, 722-727. https://doi.org/10.1134/S0036024414040177

[11] Wang, Y. and Perdew, J.P. (1992) Pair-Distribution Function and Its Coupling-Constant Average for the Spin-Polarized Electron Gas. *Physical Review B*, 46, 12947-12954. https://doi.org/10.1103/PhysRevB.46.12947

[12] Giannozzi, P., Giannozzi, P., Baroni, S., Bonini, N., Calandra, M., Car, R., *et al.* (2009) QUANTUM ESPRESSO: A Modular and Open-Source Software Project for Quantum Simulations of Materials. *Journal of Physics: Condensed Matter*, 21, Article ID: 395502. https://doi.org/10.1088/0953-8984/21/39/395502

[13] Martins, J.L. and Troullier, N. (1991) Efficient Pseudopotentials for Plane-Wave Calculations. *Physical Review B*, 43, 1993-2006. https://doi.org/10.1103/PhysRevB.43.1993

[14] Heyd, J., Peralta, J.E. and Scuseria, G.E. (2005) Energy Band Gaps and Lattice Parameters Evaluated with the Heyd-Scuseria-Ernzerhof Screened Hybrid Functional. *The Journal of Chemical Physics*, 123, Article ID: 174101.

https://doi.org/10.1063/1.2085170

[15] Perdew, J.P. and Burke, K. (1996) Comparison Shopping for a Gradient-Corrected Density Functional. *International Journal of Quantum Chemistry*, **57**, 309-319. https://doi.org/10.1002/(SICI)1097-461X(1996)57:3<309::AID-QUA4>3.0.CO;2-1

[16] Heyd, J. and Scuseria, G.E. (2006) Spin-Orbit Splittings and Energy Band Gaps Calculated with the Heyd-Scuseria-Ernzerhof Screened Hybrid Functional. *The Journal of Chemical Physics*, **124**, Article ID: 219906. https://doi.org/10.1063/1.2204597

[17] Van De Walle, C.G. and Janotti, A. (2007) The Perdew-Burke-Ernzerhof Exchange-Correlation Functional Applied to the G2-1 Test Set Using a Plane-Wave Basis Set. *Physical Review B*, **75**, Article ID: 121201.

[18] Gallino, F. and Valentin, C.D. (2011) Copper Impurities in Bulk ZnO: A Hybrid Density Functional Study. *The Journal of Chemical Physics*, **134**, Article 144506. https://doi.org/10.1063/1.3575198

[19] Debbichi, L., Said, M., Debbichi, M. and Sakhraoui, T. (2013) Hybrid Functional Study of Structural, Electronic and Magnetic Properties of S-Doped ZnO with and without Neutral Vacancy. *Journal of Alloys and Compounds*, **578**, 602-608. https://doi.org/10.1016/j.jallcom.2013.06.121

[20] Hummer, K., Harl, J. and Kresse, G. (2009) Heyd-Scuseria-Ernzerhof Hybrid Functional for Calculating the Lattice Dynamics. *Physical Review B*, **80**, Article 115205. https://doi.org/10.1103/PhysRevB.80.115205

[21] Carlo, A. and Barone, V. (1999) Toward Reliable Density Functional Methods without Adjustable Parameters: The PBE0 Model. *The Journal of Chemical Physics*, **110**, 6158-6170. https://doi.org/10.1063/1.478522

[22] Vollstädt, H., Ito, E., Akaishi, M., Akimoto, S. and Fukunaga, O. (1990) High-Pressure Synthesis of Rock-Salt Type of AlN. *Proceedings of the Japan Academy, Series B*, **66**, 7-9. https://doi.org/10.2183/pjab.66.7

[23] Berkok, H., *et al.* (2013) Structural and Electronic Properties of ScxAl1-xN: First Principles Study. *Physica B: Condensed Matter*, **411**, 1-6. https://doi.org/10.1016/j.physb.2012.11.035

[24] Schulz, H. and Thiemann, K.H. (1977) Crystal Structure Refinement of AlN and GaN. *Solid State Communications*, **23**, 815-819. https://doi.org/10.1016/0038-1098(77)90959-0

[25] Höglund, C., Bareño, J., Birch, J., Alling, B., Czigány, Z. and Hultman, L. (2009) Cubic ScAlN Solid Solution Thin Films Deposited by Reactive Magnetron Sputter Epitaxy onto ScN(111). *Journal of Applied Physics*, **105**, Article ID: 113517. https://doi.org/10.1063/1.3132862

[26] Feng, W., *et al.* (2010) Phase Stability, Electronic and Elastic Properties of ScN. *Physica B: Condensed Matter*, **405**, 2599-2603. https://doi.org/10.1016/j.physb.2010.03.042

[27] Höglund, C., Birch, J., Alling, B., Bareño, J., Czigány, Z., *et al.* (2010) Wurtzite Structure Sc$_{1-x}$Al$_x$N Solid Solution Films Grown by Reactive Magnetron Sputter Epitaxy: Structural Characterization and First-Principles Calculations. *Journal of Applied Physics*, **107**, Article ID: 123515. https://doi.org/10.1063/1.3448235

[28] Yang, J.-F., Jiao, Z.-Y. and Ma, S.-H. (2011) A Comparison of the Electronic and Optical Properties of Zinc-Blende, Rocksalt and Wurtzite AlN: A DFT Study. *Solid State Sciences*, **13**, 331-336. https://doi.org/10.1016/j.solidstatesciences.2010.11.030

[29] Zhang, X., Chen, Z., Zhang, S., Liu, R., Zong, H., Jing, Q., Li, G., Ma, M. and Wang,

W. (2007) Electronic and Optical Properties of Rock-Salt Aluminum Nitride Obtained from First Principles. *Physics of Condensed Matter*, **19**, Article ID: 425231. https://doi.org/10.1088/0953-8984/19/42/425231

[30] Devreese, J.T., Van Camp, P.E. and Van Doren, V.E. (1991) High-Pressure Properties of Wurtzite- and Rocksalt-Type Aluminum Nitride. *Physical Review B*, **44**, 9056-9059. https://doi.org/10.1103/PhysRevB.44.9056

[31] Medraj, M., Baik, Y., Thompson, W.T. and Drew, R.A.L. (2005) Understanding AlN Sintering through Computational Thermodynamics Combined with Experimental Investigation. *Journal of Materials Processing Technology*, **161**, 415-422. https://doi.org/10.1016/j.jmatprotec.2004.05.031

[32] El-Hasan, M., Abu-Jafar, M.S. and Abu-Labdeh, A.M. (2010) The Energy Band Gap of ScN in the Rocksalt Phase Obtained with LDA/GGA+ USIC Approximations in FP-LAPW Method. *Computational Materials Science*, **50**, 269-273. https://doi.org/10.1016/j.commatsci.2010.07.001

[33] Mancera, L., López, W.P. and Rodríguez, J. (2009) In-Composition Effect on Band Gap Width of $Sc_{1-x}In_xN$ Alloys. *Journal of Alloys and Compounds*, **481**, 697-703. https://doi.org/10.1016/j.jallcom.2009.03.076

[34] Jiang, H., Gomez-Abal, R.I., Rinke, P. and Scheffler, M. (2010) First-Principles Modeling of Localized States with the Approach. *Physical Review B*, **82**, Article ID: 045108. https://doi.org/10.1103/PhysRevB.82.045108

[35] Kordesch, M.E. and Little, M.E. (2001) Band-Gap Engineering in Sputter-Deposited ScGaN. *Applied Physics Letters*, **78**, 2891-2892. https://doi.org/10.1063/1.1370548

[36] Zhang, S. and Moram, M.A. (2014) ScGaN and ScAlN: Emerging Nitride Materials. *Journal of Materials Chemistry A*, **2**, 6042-6050. https://doi.org/10.1039/C3TA14189F

[37] Said, A., Debbichi, M. and Said, M. (2016) Theoretical Study of Electronic and Optical Properties of BN, GaN and $B_xGa_{1-x}N$ in Zinc Blende and Wurtzite Structures. *Optik—International Journal for Light and Electron Optics*, **127**, 9212-9221. https://doi.org/10.1016/j.ijleo.2016.06.103

[38] Nishio, M., Guo, Q., Ogawa, H. and Yoshida, A. (1997) Optical Properties of Aluminum Nitride. *Physical Review B*, **55**, R15987-R15988. https://doi.org/10.1103/PhysRevB.55.R15987

[39] Saha, B., Naik, G., Drachev, V.P., Boltasseva, A., Marinero, E.E. and Sands, T.D. (2013) Thermal and Thermoelectric Properties of Nitride Metal/Semiconductor Superlattices. *Journal of Applied Physics*, **114**, Article ID: 063519. https://doi.org/10.1063/1.4817715

[40] Bechstedt, F. and Karch, K. (1997) *Ab Initio* Lattice Dynamics of BN and AlN: Covalent Versus Ionic Forces. *Physical Review B*, **56**, 7404-7415. https://doi.org/10.1103/PhysRevB.56.7404

[41] Wilkins, J.W., Chen, J. and Levine, Z.H. (1995) Calculated Second-Harmonic Susceptibilities of BN, AlN, and GaN. *Applied Physics Letters*, **66**, 1129-1131. https://doi.org/10.1063/1.113835

[42] Pan, L., Lu, T.C., Su, R., *et al.* (2012) Study of Electronic Structure and Optical Properties of γ-AlON Crystal. *Acta Physica Sinica*, **61**, Article ID: 027101. https://doi.org/10.7498/aps.61.027101

[43] Huang, K. (1988) on Recent Developments of Semiconductor Superlattices and Quantum Wells. *Wuli* (*Physics*), **17**, 385-392. (In Chinese)

[44] Shen, X.C. (1992) The Spectrum and Optical Property of Semiconductor. Science

Press, Beijing, 76.

[45] Cheng, Y.C., Wu, X.L., Zhu, J., Xu, L.L., Li, S.H. and Chu, P.K. (2008) Optical Properties of Rocksalt and Zinc Blende AlN Phases: First-Principles Calculations. *Journal of Applied Physics*, **103**, Article ID: 073707. https://doi.org/10.1063/1.2903138